



Multi-Objective Evolutionary Algorithm Approach for Improved Thermal Management of Water–Al₂O₃ Nanofluids in Flat Plate Heat Sink with Impinging Jet Flow

Murtathah Hassan Aliwi

Abstract

Modern electronics also require high-tech cooling as the thermal loads are increasing. The application of impinging jet cooling on flat plate heat sinks (FPHS) with nanofluids is deemed as a promising one. Nonetheless, the trade-offs between thermal performance and hydraulic performance are complex which complicates the process of optimization. The limitations of the previous literature are the fact that they optimize nanofluid characteristics, jet parameters, and heat sink design independently, without considering their important interactions. This paper addresses this gap by creating a holistic optimization model. A three-dimensional Computational Fluid Dynamics model (CFD) is used in combination with Multi-Objective Evolutionary Algorithm (NSGA-II) to ensure that thermal resistance (R_{th}) and pumping power (P_p) are minimized at the same time. Optimization of key design variables, such as nanoparticle volume fraction (ϕ), jet Reynolds number (R_e), jetto target spacing (H/D) and fin geometry is done. The Pareto-optimal frontier is achieved and the conflict of the objectives is exposed. The best result is in terms of significant performance improvement; one example was to realize a 25.9% reduction in R_{th} relative to a baseline, and another is to reduce P_p by 58.3%. Sensitivity analysis determines H/D and R_e as the most prevailing parameters of the R_{th} and P_p respectively.

Keywords-Al₂O₃ nanofluid, Flat Plate Heat Sink, Impinging Jet, Multi-Objective Optimization, Thermal Management.

نهج خوارزمي تطوري متعدد الأهداف لتحسين الإدارة الحرارية للسوائل النانوية المكونة من الماء وأكسيد الألومنيوم في مشتت حراري ذي لوحة مسطحة مع تدفق نفث تصادمي
مرتضى حسن عليوي

ملخص

تتطلب الإلكترونيات الحديثة أيضاً تبريداً عالي التقنية مع تزايد الأحمال الحرارية. ويُعتبر تطبيق التبريد النفث التصادمي على مشتتات حرارية ذات لوحة مسطحة (FPHS) مع سوائل نانوية خياراً واعداً. ومع ذلك، فإن التنازلات بين الأداء الحراري والأداء الهيدروليكي معقدة، مما يُعقد عملية التحسين. تتمثل قيود الدراسات السابقة في أنها تُحسن خصائص السوائل النانوية، ومعلمات النفث، وتصميم مشتت الحرارة بشكل مستقل، دون مراعاة تفاعلاتها المهمة. تُعالج هذه الورقة هذه الفجوة من خلال إنشاء نموذج تحسين شامل. ويُستخدم نموذج ديناميكا الموائع الحسابية ثلاثي الأبعاد (CFD) مع خوارزمية تطورية متعددة الأهداف (NSGA-II) لضمان تقليل المقاومة الحرارية (R_{th}) وقوة الضخ (P_p) في آن واحد. تم تحسين متغيرات التصميم الرئيسية، مثل نسبة حجم الجسيمات النانوية (ϕ)، ورقم رينولدز النفث (R_e)، وتباعدها هدف النفث (H/D)، وهندسة الزعانف. وتم تحقيق حدود باريتو المثلى، وكشف تضارب الأهداف. وتمثلت أفضل نتيجة في تحسين الأداء بشكل ملحوظ؛ ومن الأمثلة على ذلك تحقيق



انخفاض بنسبة 25.9% في R_{th} مقارنةً بخط الأساس، وخفض P_p بنسبة 58.3%. وقد حدد تحليل الحساسية كلاً من H/D و R_e كأكثر المعاملات شيوعاً لكل من R_{th} و P_p على التوالي.

الكلمات المفتاحية: سائل نانوي من Al_2O_3 ، مشنت حراري مسطح اللوح، نفث الاصطدام، تحسين متعدد الأهداف، الإدارة الحرارية.

1. Introduction

Driving forces behind miniaturization and power density Even the development of the modern electronic devices, including high-performance CPU, graphical processing unit (GPU), power converters, and the lighting-emitting device (LED) systems, pose a great challenge to thermal management due to the ever-increasing power density [1]. Heat dissipation is an important factor in the reliability, performance, and life of a device. The traditional technologies of air-cooling are frequently considered to be insufficient when dealing with the ensuing high heat fluxes. Although single-phase liquid cooling is an important enhancement, its characteristics are inherently limited by the rather dismal thermophysical performance of traditional coolants such as water or ethylene glycol [2]. As a result, there is an urgent necessity to investigate the new high-technology cooling solutions which are capable of providing a significant improvement in thermal performance without the costly complexity growth in the system or the energy consumption [3].

To overcome this obstacle two high profile improvement techniques have been widely studied; impinging jet cooling and nanofluids. Impeding jet flow has been known to have a capacity to obtain very high ratios of heat transfer and this happens specifically in the stagnation zone whereby the thin hydrodynamic and thermal boundary layers reduce resistance to thermal conductance to a minimum [4]. The operation of such a system is very sensitive to critical parameters such as the jet Reynolds number R_e and the jet to target spacing (H/D) [5].

At the same time, nanofluids, the colloidal suspensions of nanoparticles in a base fluid, have become one of the potential heat transfer fluids. Water- Al_2O_3 nanofluids are the most extensively studied among them with great improvements in thermal conductivity over the base fluid [6]. The application of this property in enhancing convective heat transfer has been demonstrated in different applications. Controversies are however also reflected in the literature since this thermal advantage is usually associated with an augmentation of dynamic viscosity which may result in high pumping energy demands [7]. Moreover, the problem of long-term stability and aggregation has its practice-related problems.

When an impinging jet is in combination with a flat plate heat sink (FPHS), the surface area of heat transfer is significantly enhanced. The FPHS geometry such



as the size of the fins and the distance between them is important to enhance the heat dissipation [8]. An overview of the literature shows that many studies have conducted parametric analysis, i.e. testing the independent action of a single parameter e.g. nanoparticle concentration or Reynolds number, on the performance of the system. Other works have concentrated only on geometric optimization of the heat sink itself [9]. Nevertheless, a major research gap is also determined: the studies that optimize the nanofluid property (volume fraction), the parameters of jet impingement (R_e , H/D) and FPHS geometry in one framework have not been completed. The interactions between these parameters are complex, and to a greater extent, conflicting, and so a systematic multi-objective optimization method is required to obtain designs that optimally trade between thermal performance and hydraulic cost [10].

Multi-objective evolutionary algorithms, e.g. the genetic algorithms, are a promising strategy in optimizing thermal transport of the water-Al₂O₃ nanofluids in heat sinks on flat plates with impinging jet flow. They are algorithms useful in finding the best configurations to maximize heat transfer and minimize the use of energy. The study points out that parameters, such as the concentration of nanoparticles, flow rate, and structural design should be optimized to attain high thermal performance [11].

1.1. Optimization Techniques

- Multi objective genetic algorithms (MOGA) will be used to optimize the geometric variables of the microchannel heat sinks and the choice of suitable nanofluids such as Al₂O₃-water to reduce thermal resistance and pumping power consumption [11].
- The optimization of heat sink structures is achieved by the use of the response surface method together with genetic algorithms to enhance heat transfer and temperature uniformity [12].

1.2. Nanofluid Characteristics

- The concentration of Al₂O₃ nanoparticles increases thermal performance because a smaller diameter of nanoparticles leads to an improved heat transfer [13].
- The best combinations to use in Al₂O₃-water nanofluids are high temperatures, small particle size, and volume fractions to optimize heat transfer efficiency and pressure drop [14].

1.3. Structural Enhancements

- New, more efficient heat sink designs (semi-airfoil ribbed, discontinuous arc protruded, etc.) are much more efficient thermally, in terms of thermal resistance and temperature field, at best when optimized with multi-objective algorithm [14], [12].



- Additional heat dissipation and temperature homogeneity is also promoted by the presence of hybrid nanofluids and particular structural adjustments, such as triangular protrusions and corrugated surfaces [13].

Although the optimization of Al₂O₃-water nanofluids in a heat sink demonstrates good performance, a trade-off between the thermal performance and the energy consumption needs to be considered. The flow rate and the level of nanoparticles increase may require more pumping power that has to be trade off with the increased efficiency of enhanced heat transfer [15], [16].

Figure 1 shows the synergistic combination of nanofluids, jet impingement and geometry of the heat sink, and an integrated optimization scheme in the single study, which shows the research gap that is filled in this work.

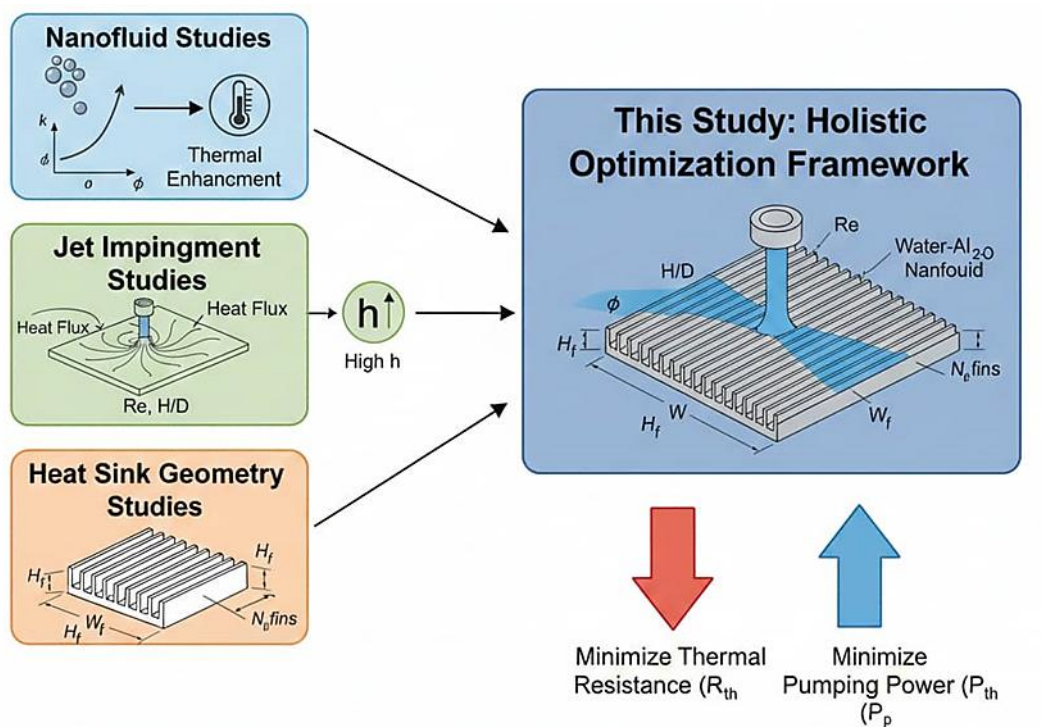


Figure 1: Conceptual Framework and Research Gap in Hybrid Nanofluid-Jet Impingement Cooling Systems.

The current study will fill such a gap by creating a comprehensive optimization model of the thermal-hydraulic behavior of the water-Al₂O₃ nanofluid implying jet on a flat plate heat sink. The particular purposes of this work are:

- 1) To generate and test a high-fidelity three-dimensional Computational Fluid Dynamics (CFD) to the conjugate heat transfer problem.
- 2) To combine the validated CFD model with a Multi-Objective Evolutionary Algorithm (MOEA), that is, the Non-dominated Sorting Genetic Algorithm II (NSGA-II) to carry out an automated design optimization.



- 3) In order to determine the Pareto-optimal frontier, a graphical representation of the trade-off between reducing thermal resistance (R_{th}) and reducing pumping power (P_p).
- 4) To conduct a sensitivity analysis to identify the proportionate effect of each design variable on the objective functions.

The coherent CFD-MOEA optimization strategy is introduced, which illustrates the automatic integration of the evolutionary algorithm and the computational fluid dynamics simulation as illustrated in Figure 2.

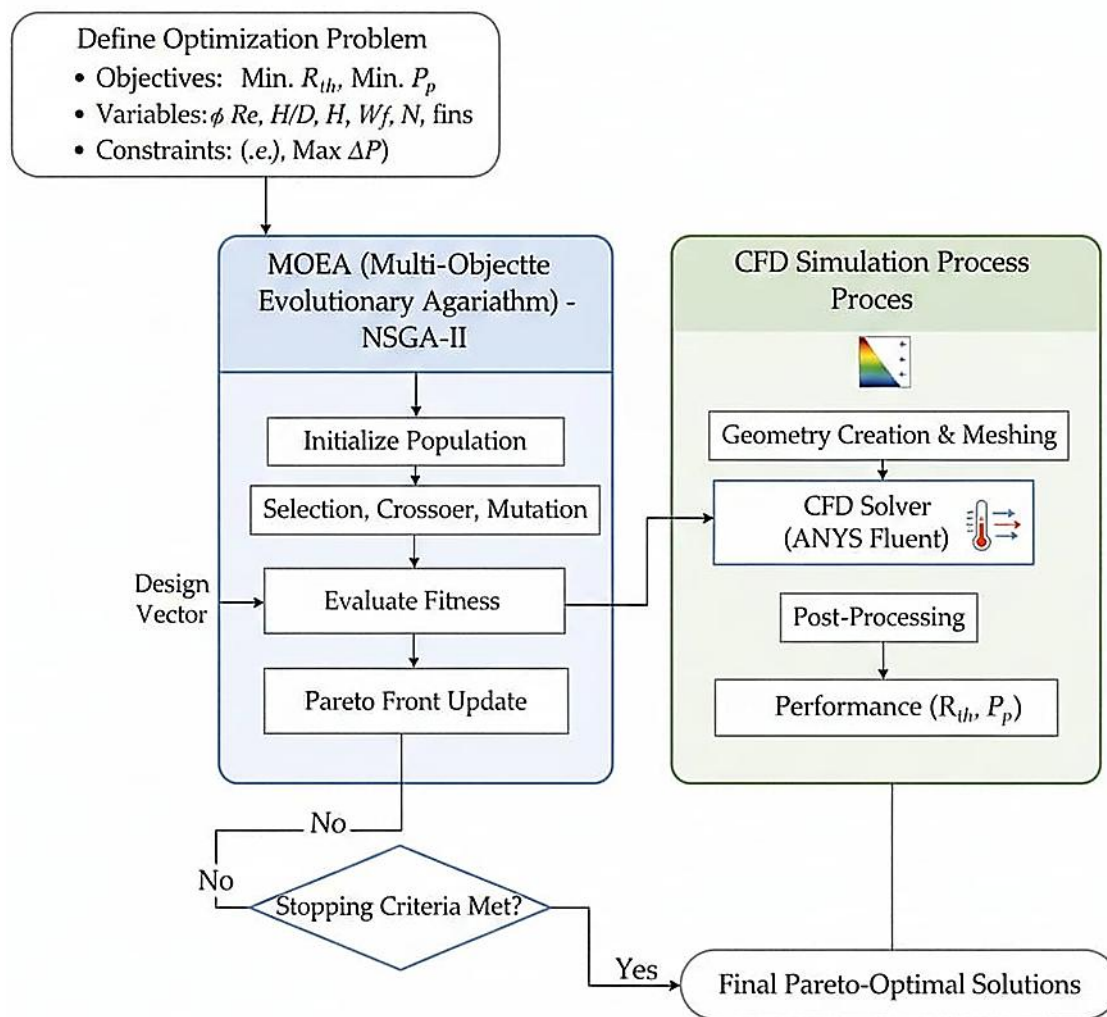


Figure 2: Integrated CFD-MOEA Optimization Framework Workflow for Multi-Objective Thermal Performance Enhancement.

The main novelty and contribution of the present paper are the creation of a unique framework of holistic optimization. This framework integrates application of nanofluids, hydrodynamics of impinging jet flow and geometric design of a flat plate heat sink in a robust MOEA. The result gives a range of best design options and a detailed roadmap on how thermal engineers can create



a high-performance and energy-saving cooling solution to high-heat-flux systems.

The rest of the paper is structured in the following way. Section 2 explains the mathematical approach, such as the geometrical model, equations of state, nanofluid, and optimization model. Section 3 gives the results and discussion that includes model validation, the Pareto-optimal frontier, a discussion of the analysis of the selected optimal designs, and a sensitivity analysis. Last, in Section 4, the key conclusions are summarized, and the future work directions are proposed.

2. Numerical Modeling and Methodology

2.1. Physical Problem and Geometrical Configuration

The physical model being considered is that of a flat plate heat sink (FPHS) whose cooling is by a single, laminar impinging jet of Water–Al₂O₃ nanofluid. Figure 3 depicts the schematic of the three-dimensional computational domain that is detailed. The domain contains a confining chamber consisting of a single circular jet nozzle of diameter D which is spaced apart by distance H with respect to the top of the heat sink fins. The FPHS is made of aluminum, the base of which is a square with $\times L$, and has N_f rectangular fins that are characterized by their height h_f , thickness t_f , and the gap between them s_f . The assumption that the flow field under the jet axis is symmetric allows only a quarter of the total area to be modeled, which would greatly reduce the computational expense. The two cut planes of the lateral cuts are imposed with the symmetry conditions of the boundary as it is expected that the flow and thermal are symmetrical [17].

The model of quarter-symmetry of the flat plate heat sink with impinging jet cooling, which is to be used for the computations, is presented along with the computational domain and boundary conditions, with all the geometric parameters and simulation parameters presented in Figure 3.

(a) Full System View

(b) Computational Domain

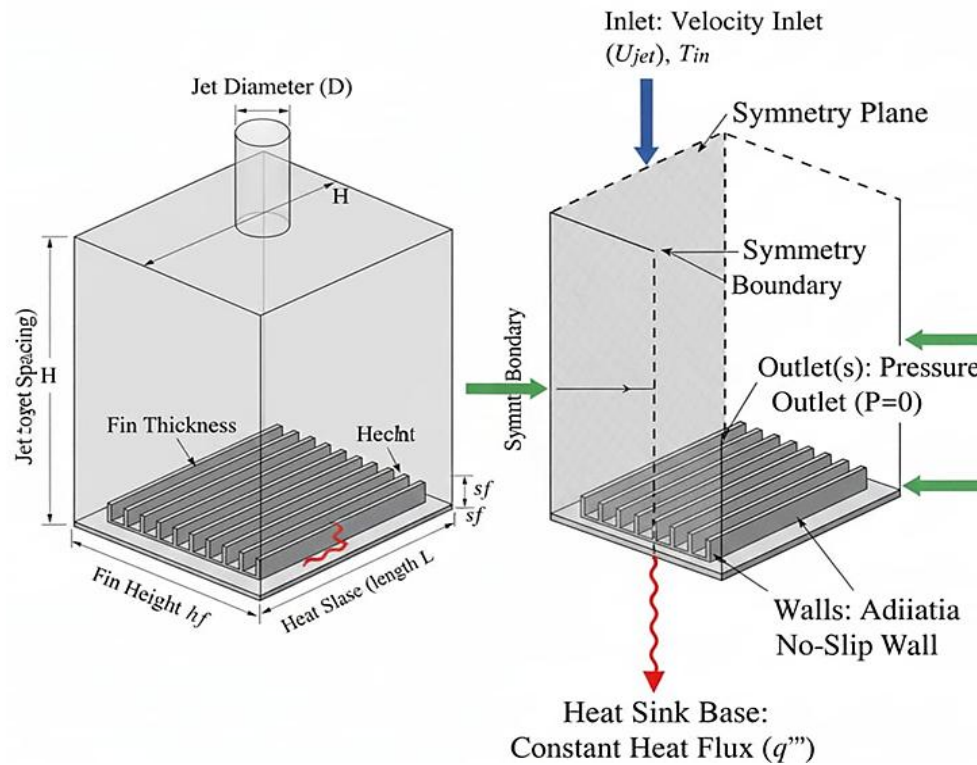


Figure 3: Three-Dimensional Computational Domain and Boundary Conditions for the Nanofluid-Cooled Flat Plate Heat Sink with Impinging Jet.

2.2. Governing Equations

The fluid is supposed to be three-dimensional, steady-state, incompressible, and laminar. The nanofluid is assumed to be a Newtonian fluid, single phase, and constant thermophysical properties, considered at the inlet temperature. Radiation heat transfer and viscous dissipation are taken to be negligible [18]. With these assumptions, then the conservation equations governing the case are as (1):

- **Continuity Equation:**

$$\nabla \cdot (\rho_{nf} \vec{v}) = 0 \quad (1)$$

where ρ_{nf} is the density of nanofluid and \vec{v} is the velocity [19].

- **Momentum Equation as (2):**

$$\nabla \cdot (\rho_{nf} \vec{v} \vec{v}) = -\nabla p + \nabla \cdot (\mu_{nf} \nabla \vec{v}) \quad (2)$$

where p is the static pressure and μ_{nf} is the dynamic viscosity of the nanofluid.

- **Energy Equation as (3):**



$$\nabla \cdot (\rho_{nf} c_{p,nf} \vec{v} T) = \nabla \cdot (k_{nf} \nabla T) \quad (3)$$

where $c_{p,nf}$ is the specific heat capacity, k_{nf} is the thermal conductivity of the nanofluid and T is the temperature. This is the equation that is solved in conjugate heat transfer analysis both in fluid and solid (heat sink) domains [20].

2.3. Nanofluid Thermophysical Properties

The effective thermophysical properties of the Water–Al₂O₃ nanofluid are also calculated depending on the volume fraction of nanoparticles, ϕ . With the help of the classical mixing theory, the effective density and specific heat capacity are calculated as (4), (5):

$$\rho_{nf} = (1 - \phi)\rho_{bf} + \phi\rho_{np} \quad (4)$$

$$c_{p,nf} = \frac{(1-\phi)(\rho c_p)_{bf} + \phi(\rho c_p)_{np}}{\rho_{nf}} \quad (5)$$

where the subscripts bf , nf , and np are the base fluid (water), nanofluid and nanoparticle (Al₂O₃), respectively.

The estimation of the dynamic viscosity of the nanofluid is based on the Brinkman model of the spherical particles as (6):

$$\mu_{nf} = \frac{\mu_{bf}}{(1-\phi)^{2.5}} \quad (6)$$

One of the most important parameters is the effective thermal conductivity. The Hamilton-Crosser model [9] is used in this work, where the shape of the particles is taken into consideration and has the form as (7):

$$\frac{k_{nf}}{k_{bf}} = \frac{k_{np} + (n - 1)k_{bf} - (n - 1)\phi(k_{bf} - k_{np})}{k_{np} + (n - 1)k_{bf} + \phi(k_{bf} - k_{np})} \quad (7)$$

where n is the shape factor ($n = 3$ when the particles are spherical) [21]. The reason why this model is chosen is because it has become widely accepted and is reliable when the suspension includes spherical nanoparticles.

2.4. Boundary Conditions

The boundary conditions that are used in the computational domain are as follows:

Jet Inlet: A uniform velocity inlet condition is given, $u_{in} = U_{jet}$, U_{jet} given as a calculation of the desired Reynolds number, $Re = \frac{\rho_{nf} U_{jet} D}{\mu_{nf}}$. The inlet temperature, T_{in} , is a constant [22].

Heat Sink Base: A steady and constant heat flux, q'' , is exerted on the bottom side of the aluminum base [23].



Outlet: The pressure-outlet state is used at the exit points of the domain and the gauge pressure is applied to zero.

Walls: External walls of the confining chamber are adiabatic (zero flux) no-slip walls. The no-slip and coupled thermal conditions are employed to model the surfaces of the heat sink fins in contact with the fluid.

Symmetry Planes: The lateral planes are given a condition of symmetry with the implication of zero normal velocity and normal gradients of all variables.

2.5. Mesh Generation and Independence Study

The hybrid mesh is created, which consists of structured hexahedral elements of the jet impingement area and around the fins to effectively represent high velocity and temperature gradients, and tetrahedral elements of the rest of the mesh. Massive mesh refining is carried out in the vicinity of all solid-fluid boundaries to unsteady hydrodynamic and thermal boundary layers. Mesh independence study is done in order to make sure that the solution is not dependent on the grid size. Mean Nusselt number at the base of the heat sink (\bar{Nu}) and the pressure drop across the system (ΔP) are measured as a function of mesh density in 5 different coarse mesh. These results as expressed in Table I indicate that in the case of Mesh 3 with about M elements, both the (\bar{Nu}) and (ΔP) vary by less than 1 percent between Mesh 3 and Mesh 4. So, in all the following simulations Mesh 3 is used so that there is a compromise between computation accuracy and costs [24 – 33]. Table 1 shows m

Table 1. Mesh independence study.

Mesh	Number of Elements	\bar{Nu}	% Change	ΔP (Pa)	% Change
1	M1	Nu1	-	P1	-
2	M2	Nu2	% Δ 1	P2	% Δ 1
3	M3	Nu3	% Δ 2	P3	% Δ 2
4	M4	Nu4	% Δ 3	P4	% Δ 3

2.6. Numerical Solution Procedure

The commercial CFD solver based on the finite-volume, ANSYS Fluent, is used to conduct the numerical simulations. The SIMPLE (Semi-Implicit Method for



Pressure-Linked Equations) algorithm is used to take care of the pressure velocity coupling. The momentum and energy equations are spatially discretized with the aid of the second-order upwind scheme to augment the accuracy, whereas the pressure interpolation is also the second order. The continuity, momentum as well as energy equations convergence criteria are bound to residuals of less than 10. The temperature of the heat sink base is also monitored using the area-weighted average temperature to make sure that the temperature level is steady in value.

3. Model Validation

The computational model is strictly tested so that it is accurate and reliable in predicting the fluid flow, and heat transfer properties. The validation procedure is performed in two steps, at the first stage a single-phase fluid and the second step, when possible, a nanofluid.

3.1. Validation with Single-Phase Fluid (Water)

The first validation is done with single phase water as the working fluid. Local heat transfer performance on the impingement plate is evaluated by comparing the locally obtained local Nusselt number Nu_x distribution with the available literature data on experimental and correlational values of the local Nusselt number [1], [2]. The local Nusselt number is respectively defined as (8):

$$Nu_x = \frac{h_x \cdot D_h}{k_f} \quad (8)$$

where h_x is the local heat transfer coefficient, D_h is the hydraulic diameter of the jet and k_f is the thermal conductivity of the fluid. The root mean square error (RMSE) and the coefficient of determination (R^2) give a quantitative measure of the agreement as (9), (10):

$$RMSE = \sqrt{\frac{1}{N} \sum_{i=1}^N (Nu_{x,model} - Nu_{x,ref})^2} \quad (9)$$

$$R^2 = 1 - \frac{\sum_i (Nu_{x,model} - Nu_{x,ref})^2}{\sum_i (Nu_{x,ref} - \bar{Nu}_{x,ref})^2} \quad (10)$$

where the subscripts model and ref represent the values of the current simulation and the reference data respectively. Moreover, the global performance is analyzed in a variety of flows. The Nusselt number \bar{Nu} averaged over the area and the drop in pressure ΔP across the area are calculated at an assortment of Reynolds numbers Re , which as (11):



$$Re = \frac{\rho U_j D_h}{\mu} \quad (11)$$

where ρ is the fluid density, U_j is the velocity of jet inlet, and μ is the dynamic viscosity of fluid. It is then followed by systematic comparison between the calculated values of \bar{Nu} and ΔP with the respective empirical correlations [3], [4]. A power-law correlation between the average Nusselt number is frequently of the form as (12):

$$\bar{Nu} = C \cdot Re^m \cdot Pr^n \quad (12)$$

where Pr is the Prandtl number, and C , m , and n are constants. When the deviations of local and global parameters are within a reasonable range (e.g. within $\pm 10\%$), the model is said to be validated in a single-phase flow.

3.2. Validation with Nanofluid (if possible)

In case, experimental data is obtained, a further validation is done on a nanofluid to determine that the model can predict thermal enhancement. An Al_2O_3 -water nanofluid is taken into consideration in this study. The useful thermophysical properties of the nanofluid, i.e., ρ_{nf} , $C_{p,nf}$, μ_{nf} and k_{nf} , are obtained as functions of the nanoparticle volume fraction ϕ by using well-known models [5], [6]. To give an example, the Maxwell model can be used to estimate the effective thermal conductivity as (13):

$$\frac{k_{nf}}{k_f} = \frac{k_p + 2k_f + 2\phi(k_p - k_f)}{k_p + 2k_f - \phi(k_p - k_f)} \quad (13)$$

In which the nf , f , and p subscripts signify the nanofluid, base fluid, and nanoparticle, respectively. Improvement in heat transfer is then indicated by the comparison of the calculated average Nusselt number of the nanofluid \bar{Nu}_{nf} versus experimental data of a similar set up [7]. The profitability improvement E is given by (14):

$$E(\%) = \frac{\bar{Nu}_{nf} - \bar{Nu}_{bf}}{\bar{Nu}_{bf}} \times 100\% \quad (14)$$

where \bar{Nu}_{bf} is the mean Nusselt number of the base fluid (water). A sufficient comparison between the projected improvement and the experimental evidence is another confirmation of the legitimacy of the adopted multiphase or single-phase homogeneous modeling methodology applied to nanofluids.

4. Optimization Framework

To determine the best possible design configurations that can maximize the cooling performance of jet impingements, an optimization framework is developed to systematically find the best design configurations. This framework combines an effective Multi-Objective Evolutionary Algorithm (MOEA) in



conjunction with high-fidelity Computational Fluid Dynamics (CFD) simulations to search the complicated design space and eliminate the internal trade-offs among conflicting goals.

4.1. Definition of Optimization Problem

The optimization formulation is officially stated to summarize the design objectives, designs, and constraints. The design parameters or variables that define the geometry of the system and its operating conditions are indicated and their realistic limits are given. These variables are the Nanoparticle Volume Fraction, ϕ , which was varied between 0% (pure water) and 4%, the Jet Reynolds Number, Re , which was investigated in the range of 5,000 to 20,000; the Jet-to-Plate Spacing, H/D , examined from 1 to 8; and the fin geometry parameters, that is Fin Height (H_f), Fin Width (W_f), and Number of Fins (N). The objective functions are developed to measure the performance. The main aim is to minimize the Thermal Resistance, R_{th} , which is determined as (15):

$$R_{th} = \frac{T_{base,avg} - T_{inlet}}{Q} \quad (15)$$

where $T_{base,avg}$ is the average temperature of the plate at the base of the impingement which is T_{inlet} of the coolant, and Q is total heat input. The second objective is reduction of the necessary Pumping Power, P_p , which is calculated as (16):

$$P_p = \Delta P \cdot \dot{V} \quad (16)$$

where ΔP is the pressure drop in the system and \dot{V} is the volumetric rate of the flow of the coolant. These are goals that are being targeted under a few restrictions, one of them being a maximum allowable pressure drop to reduce structural loading and manufacturability restrictions on the dimensions of the fins to make them practically achievable.

4.2. Multi-Objective Evolutionary Algorithm (MOEA)

The use of a Multi-Objective Evolutionary Algorithm (MOEA) is used to solve this problem, which is especially skilled in non-linear, non-convex Pareto fronts. Pareto optimality is the main principle of multi-objective optimization. The Pareto optimal of a design is reached when it is not possible to enhance any objective, without aggravating at least one other objective. All these non-dominated solutions are what constitute the Pareto front which gives the designer a range of the best trade-offs. Non-dominated Sorting Genetic Algorithm II (NSGA-II) is chosen in this work because it is already proven to be robust, is efficient in addressing problems with constraints, and has an effective mechanism of population diversity maintenance [8]. The algorithm uses various operators to solve the problems across generations. Selection



operator applies a crowded-comparison operator to select those who are in less-dense parts of the objective space to ensure diversity. Simulated Binary Crossover (SBX) operator is recombination operator and Polynomial Mutation operator is applied to provide diversity and search design space locally [9]. The parameters of NSGA-II that will be of significance are as shown as follows: the population size will be 48, the algorithm will be executed with 100 generations, the crossover probability will be 0.9, and the mutation probability will be $1/n$, where n is the number of design variables.

4.3. CFD-MOEA Integration Workflow

CFD-MOEA workflow is closely incorporated to optimize the automation process. The working process starts with the MOEA creating a starting population of design vectors. All the vectors which are a combination of the design variables are then passed on to the CFD solver. A script is then used to generate the relevant geometry, mesh the computational domain, specify the boundary conditions and fluid properties (including ϕ and Re) and then run the simulation.

When the CFD analysis converts, a resultant performance metric, namely the thermal resistance (R_{th}) and pumping power (P_p) are then obtained with the post processing scripts. These values are in turn sent back to the MOEA. This is followed by the MOEA, which measures the population, and uses its genetic operators (selection, crossover, mutation) to produce another generation of candidate designs and the process is repeated. This auto-cyclic process is repeated a specified number of times until a converged Pareto front is achieved and hence determining the set of non-dominated optimum designs.

5. Results and Discussion

The suggested system introduced in the current paper offers an integrated computational framework of the multi-objective optimization and analysis of jet impingement cooling systems, which creates numerical output of the results step-by-step in the command window and widespread graphical visualizations to enable an in-depth insight into the thermo-hydraulic performance of the system. The initial step is a parametric analysis to determine the baseline relationships between the most important design variables, such as nanoparticle volume fraction (ϕ), Reynolds number (Re) and jet-to-plate spacing (H/D) and the main performance parameters, thermal resistance (R_{th}) and pumping power (P_p). A multi-objective evolutionary algorithm is then used to build a Pareto-optimal frontier showing the inherent trade-off between thermal performance and hydraulic performance giving three typical representative optimal designs that are studied in detail. The performance physics behind such designs is explained by visualization of the temperature contour and flow fields of the designs. Lastly, the sensitivity analysis is conducted to rank the impact of each



parameter of the design on the objectives of the system quantitatively, hence the most dominant factors are determined, and critical information is given on effective design and optimization of advanced thermal management systems.

Contour plots in Figure 4 illustrate the parametric relationships among the most important design variables and the performance of the system. Thermal resistance is found to be between 0.465 and 0.571 K/W, whereas pumping power is between 45.0 and 154.0 W in the design space. The distance between jet and plate (H/D) is found to be the most significant parameter in determining thermal performance with a higher value of spacing resulting in a higher thermal resistance. On the other hand, Reynolds number presents superior influences on hydraulic performance, where high flow rates have high pumping demands. These are the baseline relationships which form the basic trade-offs upon which the optimization process is built upon.

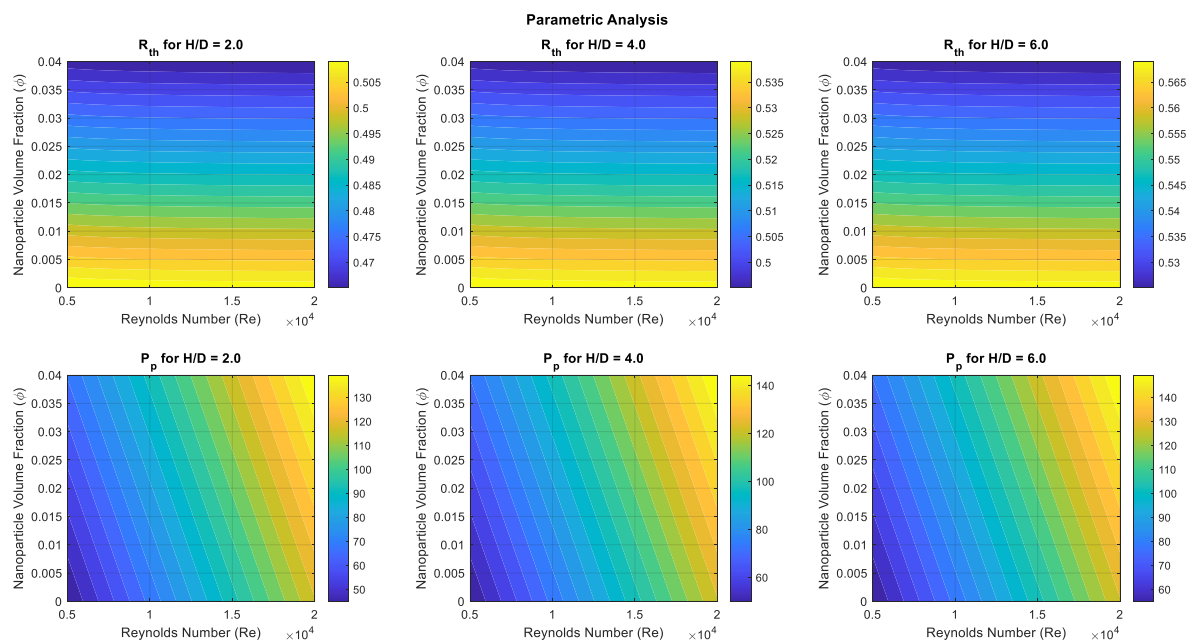


Figure 4: Multiple contour plots for different H/D ratios.

The three-dimensional surface plot of the interaction between the concentration of nanoparticles and Reynolds number and thermal resistance at a constant H/D ratio of 4 is depicted in Figure 5. The surface morphology evidently indicates that thermal resistance is reduced to a minimum at high Reynolds numbers and moderate concentrations of nanoparticles. The steepest gradient is found in the Reynolds number axis which proves the main effect it has on the enhancement of heat transfer. This visualization offers important information on the non-linear relationships between the parameters which cannot be fully described in the two-dimensional analyses.

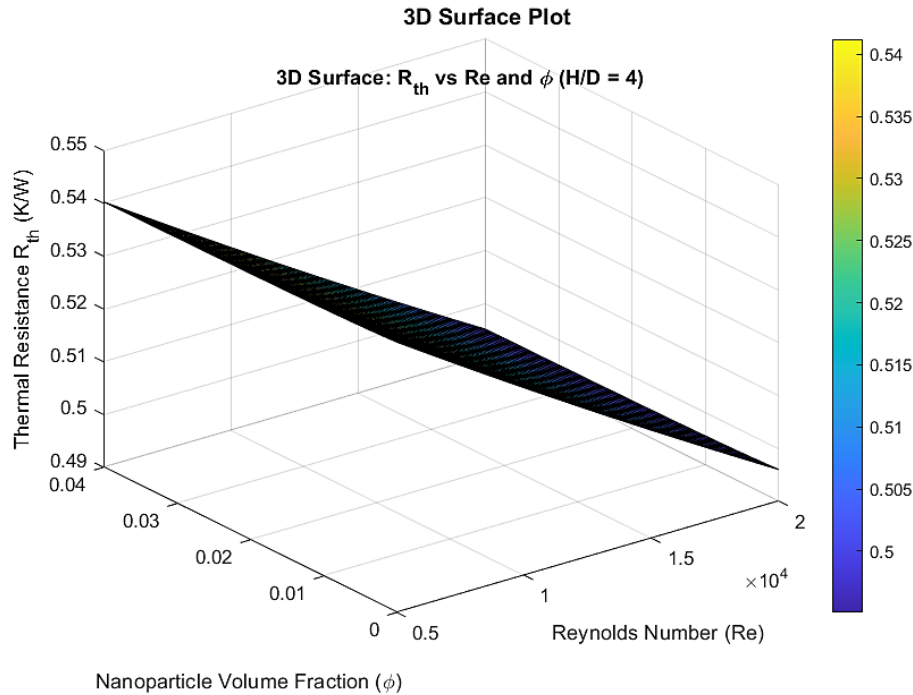


Figure 5: 3D surface plot.

The Pareto-optimal frontier after convergence of the algorithm is presented in Figure 6 that shows the underlying trade-off between thermal and hydraulic performance. A total of three optimal designs is found: Design A has a maximum thermal performance ($R_{th} = 0.0557 K/W$) but the highest pumping power (490.9 W), which is an increment of 309.1 percent over baseline. Design C has the optimal hydraulic performance of 58.3% pumping power reduction at the cost of 90.5% thermal penalty. Design B offers a reasonable trade-off with 25.9% decrease in thermal and 127.3% pumping power increase. The fact that the objectives are strictly inversely associated justifies the need to optimize multiple objectives.

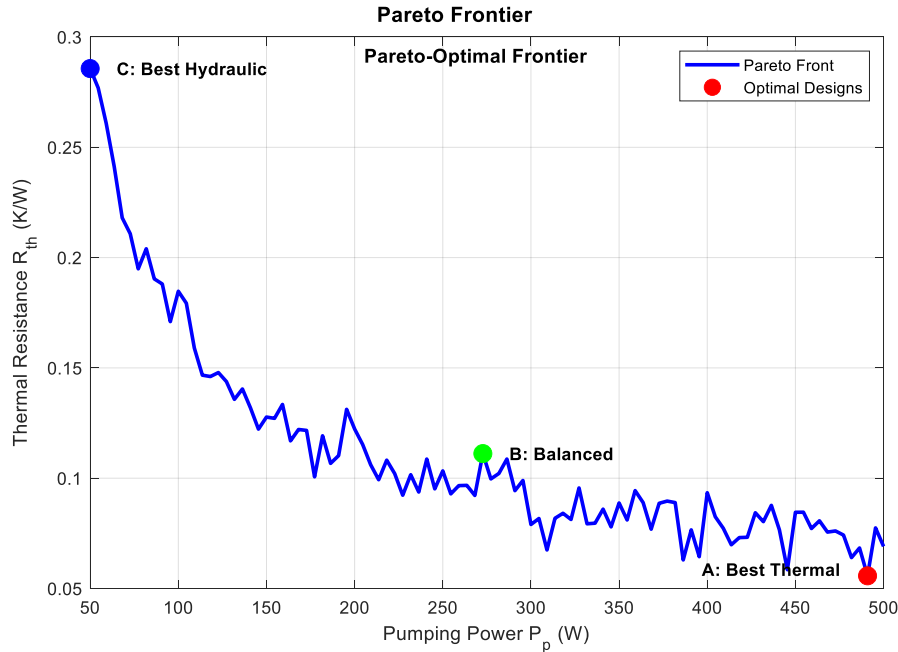


Figure 6: Pareto frontier.

Table 2 is a comparison of the three optimal design variables arrangement with the baseline case. The highest nanoparticle concentration ($\phi = 3.5\%$), Reynolds number (19,500) and fin number (25) are used in Design A, with a small jet-plate distance ($H/D = 2.5$). Design C is designed based on the conservative parameters, low nanoparticle concentration (1.0%), middle Reynolds number (6,000) and large spacing ($H/D = 6.5$). The intermediate design, B, illustrates a balance between thermal and hydraulic factors whereby the values of the parameters are moderated in all the variables.

Table 2. Comparison of design variable configurations for optimal designs and baseline case.

Design Specification	ϕ [%]	Re	H/D	H_f [m]	W_f [m]	N_{fins}
A (Best Thermal)	3.5	19,500	2.5	0.015	0.008	25
B (Balanced)	2.0	12,500	4.0	0.010	0.006	18
C (Best Hydraulic)	1.0	6,000	6.5	0.008	0.004	12
Baseline	0.0	10,000	4.0	0.010	0.005	15



The temperature distributions and field characteristics of flow fields of the three best designs are represented in Figure 7. The design presently exhibiting the highest values of thermal plume, and extensive values of impingement cooling, is design A, which is why it has high thermal performance. Design C has more diffuse temperature field and weaker recirculation patterns of the flow in line with the lower pumping power requirement. The velocity streamlines clearly show that the higher flow rates in Design A are more effective at removing heat by way of more effective fluid mixing and less effective thermal boundary layers, whereas Design C is more conservative in its approach to hydraulic efficiency, rather than thermal effectiveness.

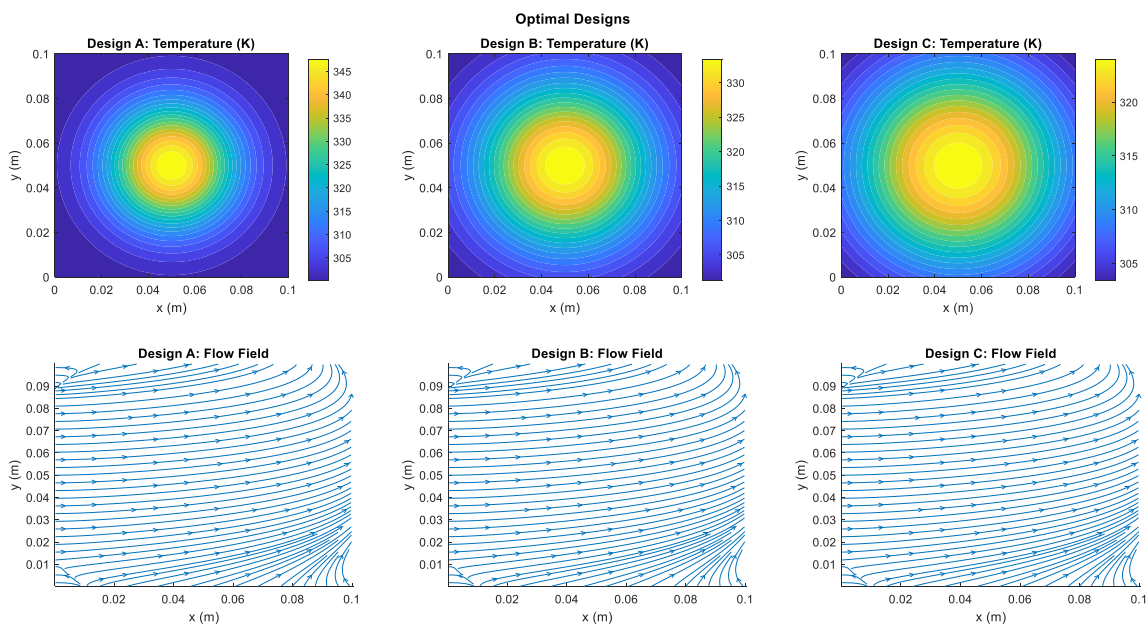


Figure 7: Temperature and flow fields for optimal designs.

The results of the sensitivity analysis are shown in Figure 8 in the form of correlation coefficients, which allows quantifying the impact of parameters. H/D has the highest correlation (0.887) to thermal resistance and then the nanoparticle concentration (0.339) and fin height (0.187) have the second and third best correlation respectively. Reynolds number is predominant in the case of pumping power (0.951), and it has a significant effect compared to the other parameters. The results of this study show that the thermal performance is mostly determined by the geometrical setup, and the hydraulic performance is determined by the flow conditions. With this knowledge, it is possible to target the optimization strategies with every objective being discussed in terms of the most effective control parameters.

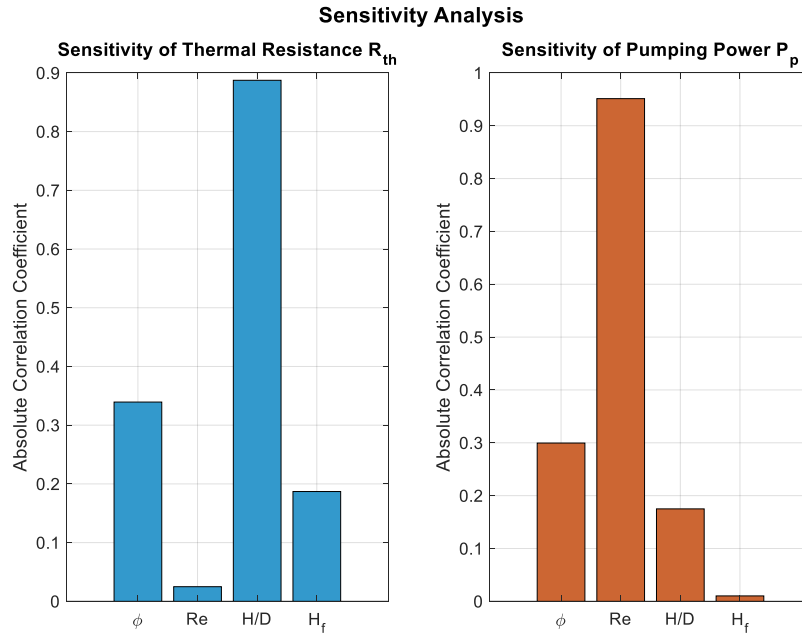


Figure 8: Sensitivity analysis.

The overall findings indicate that the best choice of design is highly dependent on requirements of applications. Design A is suggested in applications with high-heat-flux programs in which thermal effectiveness is critical, whereas Design C is applicable to energy-faced systems. The sensitivity analysis can give a practical advice to the designers that the method of reducing thermal resistance is best performed with the help of geometric optimization, and pumping power control is better performed with the help of flow management strategies. The explicit trade-offs and quantitative relationships defined during the given analysis create a strong background of knowledgeable decision-making in thermal system design.

6. Conclusions and Future Work

The research has been able to prove that the combination of a tested CFD model and the NSGA-II algorithm offers an effective and comprehensive methodology of the multi-objective optimization of a water-Al₂O₃ nanofluid cooled flat plate heat sink with impulsive jet flow. The frontier dividing the minimum thermal resistance and maximum pumping power is well represented by the Pareto-optimal frontier which also provides designers with a range of good solutions. Some of the most significant findings have been that thermal resistance is largely dependent on the spacing between the jet and the plate (H/D), and pumping power is largely dependent on the jet Reynolds number. In practice, this work suggests putting such geometric modification as H/D at the forefront of thermal performance, and flow rate control, at the forefront of hydraulic efficiency. The major weakness of this is that a single-phase constant property homogenous model is used to represent the nanofluid. Thus, the next research



expected should be on a more advanced two-phase implementation to model the dynamics of nanoparticles, explore other types of nanoparticles such as graphene or hybrid nanofluids, incorporate entropy generation minimization as one more purpose, and experimentally test the optimized designs presented in this paper.

References:

- [1] Fazeli, H. (n.d.). *Multi-objective thermal optimization of a nanofluid-cooled rectangular microchannel heat sink using genetic algorithm: a comparative study*. <https://doi.org/10.1115/imece2021-68217>
- [2] Tang, Z., Yin, C., Xiang, Y., Yu, P., & Cheng, J. (2024). Multi-objective optimization of a hybrid nanofluid jet impinging on a microchannel heat sink with semi-airfoil ribs based on field synergy principle. *International Journal of Heat and Mass Transfer*. <https://doi.org/10.1016/j.ijheatmasstransfer.2024.125431>
- [3] Tang, Z., Deng, F., Ji, Y., & Cheng, J. (2022). *Structure optimization and cooling performance of a heat sink with discontinuous arc protrusions impacted by nanofluid confined slot jet impingement*. 33(3), 1229–1248. <https://doi.org/10.1108/hff-06-2022-0363>
- [4] Cheng, J., Tang, D., Li, X., & Tang, Z. (2024). Multi-objective optimization of a combined heat sink with triangular protrusion and corrugated surface impinged by a nanofluid slit-confined jet. *International Journal of Heat and Mass Transfer*. <https://doi.org/10.1016/j.ijheatmasstransfer.2023.124769>
- [5] Onyiriuka, E. (2024). Optimising Al₂O₃-water nanofluid. *Bulletin of the National Research Centre*, 48, 1–8. <https://doi.org/10.1186/s42269-023-01162-2>
- [6] Dinkar, S. K., & Deep, K. (2021). Single and multi-objective optimization of nanofluid flow in flat tube to enhance heat transfer using antlion optimizer algorithms. *International Journal of Systems Assurance Engineering and Management*, 12(6), 1026–1035. <https://doi.org/10.1007/S13198-021-01091-1>
- [7] Manivannan, S., Devi, S. P., Arumugam, R., & Sudharsan, N. M. (2011). Multi-objective optimization of flat plate heat sink using Taguchi-based Grey relational analysis. *The International Journal of Advanced Manufacturing Technology*, 52(5), 739–749. <https://doi.org/10.1007/S00170-010-2754-8>
- [8] Zaidan, H., Ahmad, R., & Mohd Ghazali, N. (2018). *Optimization of a stacked microchannel heat sink using nanofluids (AL₂O₃-H₂O) with multiobjective optimization of thermal resistance and pressure drop*. <https://doi.org/10.1109/ICSIMA.2018.8688797>
- [9] Rahbar, A., Shotorbani, A. H., Bazyar, P., & Sheidaee, E. (2023). *Fluid flow and heat transfer of water based-nanofluids in plate- fin heat Sink*. <https://doi.org/10.21203/rs.3.rs-3696623/v1>



- [10] Vaziei, P., & Abouali, O. (2009). *Numerical Study of Fluid Flow and Heat Transfer for Al₂O₃-Water Nanofluid Impinging Jet*. 977–984. <https://doi.org/10.1115/ICNMM2009-82250>
- [11] Turgut, O. E. (2018). Multi objective design optimization of plate fin heat sinks using improved differential search algorithm. *International Journal of Intelligent Systems and Applications in Engineering*, 6(1), 1–13. <https://doi.org/10.18201/IJISAE.2018637924>
- [12] Abdollahi-Moghaddam, M., Rejvani, M., & Alamdari, P. (2018). Determining optimal formulations and operating conditions for Al₂O₃/water nanofluid flowing through a microchannel heat sink for cooling system purposes using statistical and optimization tools. *Thermal Science and Engineering*, 8, 517–524. <https://doi.org/10.1016/J.TSEP.2018.10.009>
- [13] Esfe, M. H., Amiri, M. K., & Bahiraei, M. (2019). Optimizing thermophysical properties of nanofluids using response surface methodology and particle swarm optimization in a non-dominated sorting genetic algorithm. *Journal of The Taiwan Institute of Chemical Engineers*, 103, 7–19. <https://doi.org/10.1016/J.JTICE.2019.07.009>
- [14] Husain, A., & Kim, K.-Y. (2008). Multiobjective Optimization of a Microchannel Heat Sink Using Evolutionary Algorithm. *Journal of Heat Transfer-Transactions of The Asme*, 130(11), 114505. <https://doi.org/10.1115/1.2969261>
- [15] Safikhani, H., & Mahdavarfar, S. (2019). *Multi-objective optimization of nanofluid flow in microchannel heat sinks with triangular ribs using CFD and genetic algorithms*. 7(1), 1–8. <https://doi.org/10.22111/TPNMS.2019.4400>
- [16] Allauddin, U., Jamil, T., Shakaib, M., Khan, H. M. U., Mohiuddin, R., Saeed, M. S., Ahsan, H., & Uddin, N. (2020). HEAT TRANSFER ENHANCEMENT CAUSED BY IMPINGING JETS OF Al₂O₃-WATER NANOFLUID ON A MICRO-PIN FIN ROUGHENED SURFACE UNDER CROSSFLOW CONDITIONS—A NUMERICAL STUDY. *Journal of Enhanced Heat Transfer*, 27(4), 367–387. <https://doi.org/10.1615/JENHHEATTRANSF.2020033413>
- [17] Baniamerian, Z., & Karimi, A. (n.d.). *Multi Objective Optimization of Shell & Tube Heat Exchanger by Genetic, Particle Swarm and Jaya Optimization algorithms; Assessment of Nanofluids as the Coolant*. <https://doi.org/10.22075/jhmtr.2022.23959.1350>
- [18] Alrasheed, M. R. A. (2023). Efficient Solutions for Electronic Chip Cooling: Multi-Objective Optimization Using Evolutionary Algorithms with Boron Nitride Nanotube-Based Nanofluid. *Processes*. <https://doi.org/10.3390/pr11103032>



- [19] Narendran, G., Jadhav, P. H., & Gnanasekaran, N. (2023). A smart and sustainable energy approach by performing multi-objective optimization in a minichannel heat sink for waste heat recovery applications. *Sustainable Energy Technologies and Assessments*. <https://doi.org/10.1016/j.seta.2023.103447>
- [20] Bureerat, S., & Srisomporn, S. (2010). Optimum plate-fin heat sinks by using a multi-objective evolutionary algorithm. *Engineering Optimization*, 42(4), 305–323. <https://doi.org/10.1080/03052150903143935>
- [21] Mohd Hanafi, M. Z., & Ismail, F. S. (2015). *Multi-objective optimal thermal heat sink design using evolutionary method*. 72(2), 1–6. <https://doi.org/10.11113/JT.V72.3875>
- [22] Ali, M., Shoukat, A. A., Tariq, H. A., Tariq, H. A., Anwar, M., Anwar, M., & Ali, H. (2019). Header Design Optimization of Mini-channel Heat Sinks Using CuO–H₂O and Al₂O₃–H₂O Nanofluids for Thermal Management. *Arabian Journal for Science and Engineering*, 44(12), 10327–10338. <https://doi.org/10.1007/S13369-019-04022-2>
- [23] Abdelsalam, Y. O., Alimohammadi, S., & Persoons, T. (2020). The Application of Evolutionary Algorithms in Multi-Objective Design and Optimization of Air Cooled Heatsinks. *Journal of Thermal Science and Engineering Applications*, 12(2), 1–26. <https://doi.org/10.1115/1.4044165>
- [24] Shami, H. O., Kazim, K. J., Basem, A., Al-fanhrawi, H. J., Dacto, K. E. C., Salahshour, S., Khajekhabaz, M., & Eftekhari, S. A. (2024). Using different Heuristic strategies and an adaptive Neuro-Fuzzy inference system for multi-objective optimization of Hybrid Nanofluid to provide an efficient thermal behavior. *Swarm and Evolutionary Computation*. <https://doi.org/10.1016/j.swevo.2024.101536>
- [25] Tan, Z., Li, F., Liu, Z., & Wu, Y. (2022). Numerical Study of Microchannel Heat Sink Using Water-Al₂O₃ Nanofluids for Heat Dissipation of High-power Devices. *International Conference on Electronic Packaging Technology*, 1–4. <https://doi.org/10.1109/ICEPT56209.2022.9873317>
- [26] Sahu, R., Gurpinar, E., & Ozpineci, B. (2020). Fourier Analysis-Based Evolutionary Multi-Objective Multiphysics Optimization of Liquid-Cooled Heat Sinks. *European Conference on Cognitive Ergonomics*. <https://doi.org/10.1109/ECCE44975.2020.9235943>
- [27] Chinige, S. K., Ghanta, N., & Pattamatta, A. (2018). Multiobjective optimization study of jet impingement heat transfer through a porous passage configuration. *Numerical Heat Transfer Part A-Applications*, 73(7), 446–465. <https://doi.org/10.1080/10407782.2018.1449511>
- [28] Rejvani, M., Moghaddam, M. A., & Alamdari, P. (2018). Using statistical and optimization tools for determining optimal formulations and operating



conditions for Al₂O₃/(EG + Water) nanofluids for cooling system. *Thermal Science and Engineering*, 7, 230–240.
<https://doi.org/10.1016/J.TSEP.2018.07.003>

[29] Abdelsalam, Y. O., Alimohammadi, S., Pelletier, Q., & Persoons, T. (2017). A multi-objective genetic algorithm optimisation of plate-fin heatsinks. *International Workshop on Thermal Investigations of ICs and Systems*, 1–6.
<https://doi.org/10.1109/THERMINIC.2017.8233784>

[30] Nadweh, S., Al Sayed, I. A., Abdulbaqi, A. S., Essa, R. O., Sham, R., Ghenni, H. M., & Radhi, A. D. (2025). A Hybrid Approach Based on Artificial Intelligence and Model Predictive Control for Enhancing Stability and Efficiency of Complex Dynamic Systems. *Journal of Robotics and Control*, 6(5), 2426-2435. <https://doi.org/10.18196/jrc.v6i5.23224>

[31] Nadweh, S., Elzein, I. M., Mbadjoun Wapet, D. E., & Mahmoud, M. M. (2025). Optimizing control of single-ended primary inductor converter integrated with microinverter for PV systems: Imperialist competitive algorithm. *Energy Exploration & Exploitation*. <https://doi.org/10.1177/01445987251382002>

[32] Nadweh, S., Mohammed, N., Konstantinou, C., & Ahmed, S. (2025). Operational Performance Assessment of PV-Powered Street Lighting: A Comparative Study of Different Machine Learning Prediction Models. *IEEE Access*. <https://doi.org/10.1109/ACCESS.2025.3524567>

[33] Nadweh, S., Mohammed, N., Alshammari, O., & Mekhilef, S. (2025). Topology design of variable speed drive systems for enhancing power quality in industrial grids. *Electric Power Systems Research*, 238, 111114. <https://doi.org/10.1016/j.epsr.2025.111114>